X-Ray Magneto-optics in Lanthanides

K. Starke,[1] F. Heigl,[1] A. Vollmer,[1] M. Weiss,[2] G. Reichardt,[2] and G. Kaindl[1]

[1]*Institut für Experimentalphysik, Freie Universität Berlin, Arnimallee 14, D-14195 Berlin, Germany*

[2]*BESSY, Albert-Einstein-Strasse 15, D-12489 Berlin-Adlershof, Germany*

(Received 12 April 2000)

Magneto-optical methods in the visible light regime generally lack element specificity, which has become a considerable shortcoming in research on advanced heteromagnetic systems. Using circularly polarized soft x rays tuned to a $4d$-$4f$ core-level transition of a lanthanide element, the specularly reflected x-ray intensity changes proportionally to the magnetization of this element and, e.g., hystereses are easily measured element specifically. In contrast to the case of visible light, temperature dependent $4d$-$4f$ magneto-optical signals are not influenced by the thermal lattice expansion.

DOI: 10.1103/PhysRevLett.86.3415 PACS numbers: 78.40.–q, 71.20.Eh, 85.70.Sq

Magneto-optical (MO) effects are widely known as the underlying principle of how magnetic "bits" are read from an MO disk [1], where one exploits that left- and right-hand circularly polarized light is reflected with different intensity depending on the local disk magnetization. Although MO effects are quite small in the visible-light regime, refined optical methods not only yield sufficient contrast to distinguish bits of opposite magnetization, but even allow one to observe details of magnetic domains in optical microscopes [2]. Most importantly, MO techniques are ideally suited to study the magnetization reversal process in external magnetic fields, which is impossible with, e.g., electron microscopes involving slow cascade electrons that are strongly affected by the Lorentz force. Besides all merits, conventional MO techniques lack element specificity, simply because electric dipole transitions in the visible mainly take place between delocalized valence-electron band states. This has become a severe limitation in analyzing new systems for information storage [1,3] or permanent-magnet nanostructures [4]. In these advanced magnetic systems, which are composed of several magnetic elements to compromise technical requirements, lanthanide elements (mostly Tb) are used to achieve large perpendicular magnetic anisotropy [5], and large coercive fields in spring magnets [4].

Reliable element-specific information can be obtained by techniques which involve core-level transitions, e.g., by magnetic circular dichroism in x-ray absorption (XA) [6,7]. In the soft x-ray range which is most relevant for magnetism studies, absorption signals are commonly detected by electron-yield methods [8], so that in general no large external magnetic fields can be employed, and hence no hysteresis loops have been recorded via electron yield. Alternative XA detection modes which do not employ electrons either are limited to special samples suspended on transparent foils [7] or suffer from saturation effects for all but highly diluted samples (fluorescence yield) [9]. After all, to probe magnetization reversal in external fields in an element-resolved way, it appears natural to employ x rays to reach core-level transitions and to use light reflection as in conventional magneto-optics.

Apart from their technological relevance in soft and hard magnetic films [4,5], lanthanide elements constitute a unique case in x-ray optics: the $4d \rightarrow 4f$ electric dipole transitions (so-called giant resonances) are among the strongest in the periodic table [10]. They give rise to a high absorptivity and reflectivity, corresponding to an exceptionally short x-ray absorption length of $l \approx 1$ nm [11]; it is much shorter than the lanthanide $4d \rightarrow 4f$ transition wavelength ($\lambda \approx 8$ nm), and hence $\lambda \gg l$. This unique situation is quite different from previously studied transition-metal (Fe, Co, ...) $2p \rightarrow 3d$ transitions [12,13], where attenuation lengths are much longer than the wavelength $\lambda \ll l$, leading to complicated interferences when samples are structured on the nanometer scale [13].

As a first example of a simple lanthanide system we chose an in-plane magnetized 8 nm thick gadolinium (Gd) metal film, grown *in situ* by metal vapor deposition on a single-crystal W(110) substrate [14]. Figure 1(a) shows two Gd $4d \rightarrow 4f$ absorption spectra, with the film magnetized either parallel (dotted) or antiparallel (solid curve) to the projected direction of a beam of circularly polarized (CP) synchrotron radiation [15]. Upon *magnetization reversal,* the weak pre-edge absorption lines change strongly and the broad absorption maximum near $h\nu = 149$ eV apparently shifts by over 1 eV [11]. The associated pair of x-ray reflectivity spectra is presented above in Fig. 1(b); it is recorded from the same film using a photodiode in specular geometry (see inset). For both magnetization directions, there is a pronounced maximum of 20 times higher reflected intensity than at the minimum near 136 eV; the reflectivity maxima (solid and dotted curves) are located $\sim$1.5 eV above the corresponding giant absorption peaks [Fig. 1(a)]. In the pre-edge range, only *dispersive-like* structures appear in reflectivity, with the points of steepest slope coinciding with the associated absorption peaks; this is most evident for the lowest energy line, magnified in Fig. 1(c).

All these findings are readily understood within elementary dispersion theory which formally describes the interaction of light with metals by introduction of a complex refractive index $\tilde{n} = (1 - \delta) - ik$, assuming that electrons

 © 2001 The American Physical Society

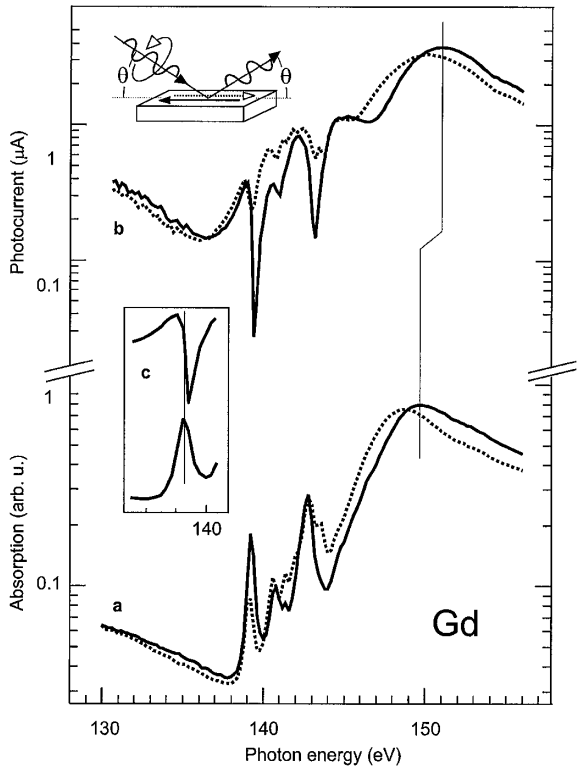

FIG. 1. (a) Gd $4d$-$4f$ absorption spectra obtained via electron yield from an 8 nm thick film with remanent in-plane magnetization parallel (dotted curve) and antiparallel (solid curve) to the (surface projected) incidence direction of a circularly polarized x-ray beam [inset of (b)]. (b) Associated spectra of specularly reflected light intensity. All spectra are recorded at $\theta = 18°$ grazing light incidence and at 25 K sample temperature. (c) The lowest energy pre-edge structure at 139.2 eV in reflection (top) and absorption (below).

are bound by elastic forces with oscillator energies equal to the optical transition energies [16]. While for normally incident light both the absorptive part k and the dispersive part δ contribute equally to the reflected intensity, the dispersive part clearly dominates at grazing incidence according to the Fresnel formulas [16]. The obvious difference in reflectivity line shapes between pre-edge and giant region [Fig. 1(b)] is simply due to the widely different transition probabilities (line strengths) in the two energy regions.

The reflected light intensity R_θ at some constant grazing angle θ [cf. inset of Fig. 1(b)] scales with the electric-dipole transition probability. It has the general property (Wigner-Eckart theorem) that, for CP-light excitation in magnetically ordered media, the difference in transition probability for oppositely magnetized samples (+ or −) is proportional to the magnetization [17]. Consequently, the difference of $4d \rightarrow 4f$ specularly reflected intensity is proportional to the $4f$-shell magnetization

$$R_\theta^+ - R_\theta^- \propto |\mathrm{M}_{4f}| . \qquad (1)$$

This simple relation holds strictly when all light is absorbed, i.e., for semi-infinite samples. However, owing to the particularly short attenuation length l near the lanthanide $4d \rightarrow 4f$ giant absorption maxima, Eq. (1) is approximately valid also for thin films and simple layered structures of lanthanide elements, as long as the thickness d of the layer containing the absorbing element clearly exceeds l. This is principally different from $2p \rightarrow 3d$ transitions in transition metals where attenuation lengths of ~20 nm usually cause substantial interference in structures of nanometer size, which inhibits the straightforward interpretation of $R_\theta^+ - R_\theta^-$ in terms of sample magnetization [13].

Unlike MO transitions in the visible-light regime [1,5], $4d \rightarrow 4f$ transition energies change significantly in going across the lanthanide series, and even neighbors in the periodic table can easily be distinguished. In Fig. 2 we compare difference reflectivity spectra of (a) Gd and (b) Tb. The Tb MO signal peaks near the Tb giant absorption at $h\nu = 157$ eV, which is several eV above the range of substantial MO signal from Gd.

In order to demonstrate the relative ease of recording element-specific hysteresis loops from heteromagnetic lanthanide systems, we fabricated an $Gd_{1-x}Tb_x$/Gd nanostructure. It was prepared by annealing a 0.3 nm Tb layer on top of a ~3 nm thick Gd film on W(110) at 1070 K; at such a high temperature, the metastable film is known to break up into large three-dimensional islands [18]. Figures 3(a) and 3(b) present hysteresis loops recorded at two different photon energies, 147 and 153 eV. By inspection of Fig. 2, we identify 147 eV with the *maximum* of the Gd spectrum and with a *node* in the Tb spectrum (energy 1); the 147 eV hysteresis thus reflects the magnetization reversal in Gd atoms only. The loop in

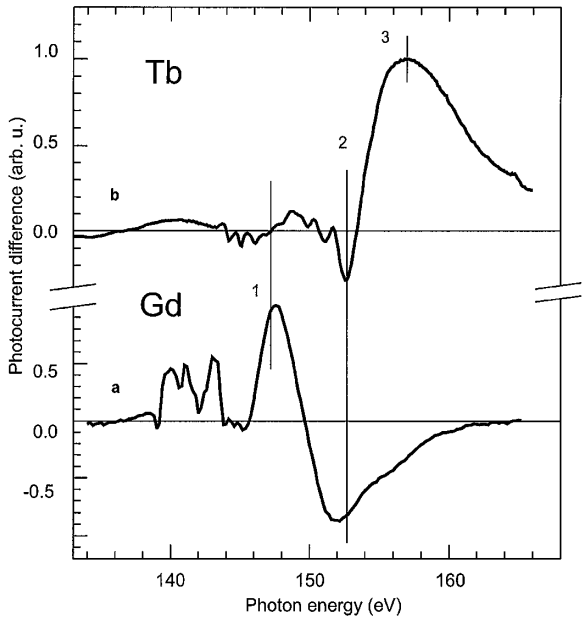

FIG. 2. (a) Difference spectrum obtained from the Gd $4d \rightarrow 4f$ reflectivity spectra in Fig. 1(b). (b) Difference spectrum of reflected intensity from an in plane magnetized Tb metal film (8 nm thick). The spectra are recorded at $\theta = 18°$ grazing light incidence ($T = 25$ K).

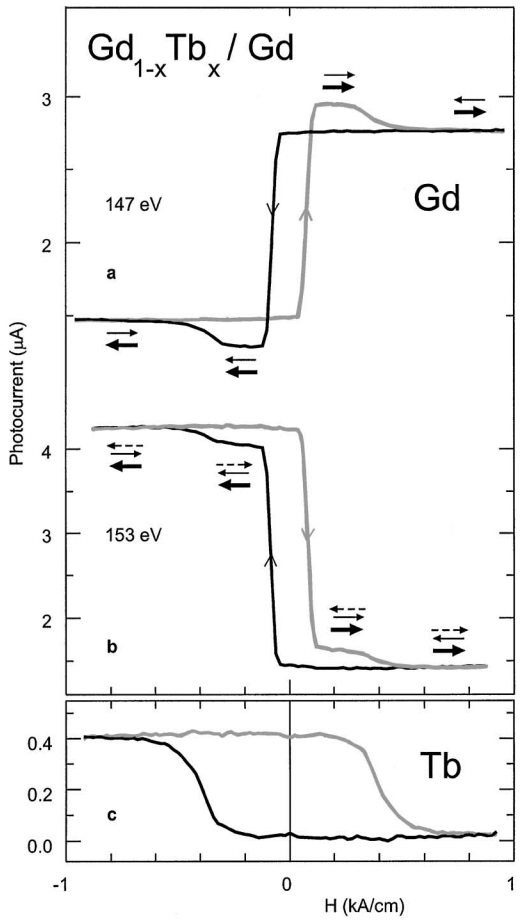

FIG. 3. Hysteresis loops of a $Gd_{1-x}Tb_x/Gd$ nanostructure at different photon energies. (a) The 147 eV loop reveals two magnetically different Gd phases. The associated magnetic orientations are indicated by big and small solid arrows. (b) The 153 eV loop reflects magnetization changes of both elements. The Tb magnetization is indicated by dashed arrows. The loops are recorded at $\theta = 18°$ grazing light incidence ($T = 25$ K). (c) The difference of the loops in (b) and (a) yields the shape of the Tb hysteresis.

Fig. 3(a) reveals two magnetically different Gd species, a magnetically soft one with low coercivity (80 A/cm) and another one in which magnetization reverses at a 5 times higher external field (400 A/cm). The overshoot clearly shows that Gd moments in these two phases are oriented *parallel* to each other for increasing fields between the two coercivities, but *antiparallel* to each other in high external fields—a quite surprising behavior at first glance. The 153 eV hysteresis [Fig. 3(b)] comprises MO signals of *both* elements (see point 2 in Fig. 2). As the 147 eV loop, it indicates that the magnetization reverses in two steps, yet there is no overshoot. In the absence of interference effects as discussed above, we obtain the shape of the magnetization-reversal curve of Tb simply by subtracting the 147 eV loop (Gd) from the one at 153 eV (superposition of Tb and Gd), with the result given in Fig. 3(c). From the element-specific Gd [Fig. 3(a)] and Tb [Fig. 3(c)] hystereses one must conclude the following: (1) it is the presence of Tb which gives rise to the magnetically harder Gd phase. (2) The surprising orientation of Gd $4f$ moments, which are antiparallel to high external fields in the magnetically hard phase, is due to an *antiferromagnetic* coupling of Gd and Tb moments in this phase, which we tentatively assign to a $Gd_{1-x}Tb_x$ alloy. In this phase, the larger Tb $4f$ moment ($9\mu_B$) dominates over the Gd $4f$ moment ($7\mu_B$) and points along high external fields; see dashed arrows in Fig. 3(b). Note that the low-coercivity Gd, which we identify with the metallic (not alloyed) phase, is not magnetically coupled to the hard magnetic phase, in agreement with the expected island structure of the film.

Another principal drawback of visible-light MO spectroscopy are thermal contributions of nonmagnetic origin to the signal. This is because valence-band energies slightly change with the thermally expanding lattice, which affects the optical constants and thus the reflected intensity of visible light. This complication often impedes a magneto-optical measurement of magnetization-versus-temperature curves, $M(T)$, particularly in lanthanide systems [19]. As an example we show visible-light MO data of a 8-nm thick Tb metal film (annealed at 650 K after deposition at room temperature [14]) in Fig. 4(a) (solid symbols). The film was cooled in an external field of opposite directions (1 kA/cm, in the film plane) from above room temperature to ~130 K. Above the ordering temperature of 220 K the signal is independent of the field direction; below it rises (drops) when the external field is parallel (antiparallel) to the projected light propagation direction [20,21]. The nonmagnetic contributions to the visible-light

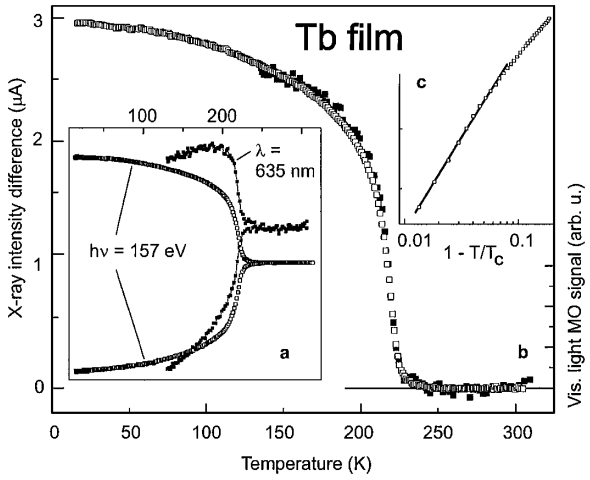

FIG. 4. Temperature dependent magnetization of an 8 nm thick Tb film. Open symbols: x-ray reflectivity ($\theta = 18°$); solid symbols: visible-light MO data ($\lambda = 635$ nm). (a) The film was cooled down in a field of 1 kA/cm of opposite directions along the film plane. (b) Magnetization curves $M(T)$, which are the difference of the associated branches in (a). (c) Double logarithmic plot of the magnetization vs the reduced temperature $t = (1 - T/T_C)$. The critical exponent is determined by a least-squares fit analysis in the range $1 \times 10^{-2} < t < 8 \times 10^{-2}$.

MO signal become very obvious below ~200 K where the slope of the upper branch even changes sign. Only the difference of the two branches reflects the magnetization curve [solid symbols in Fig. 4(b)].

Lanthanide $4d \rightarrow 4f$ transitions, by contrast, involve only core levels which do not take part in chemical bonding, and we may anticipate that changes of $4d \rightarrow 4f$ MO signal reveal changes in the $4f$ magnetization free of nonmagnetic contributions. This is indeed the case: magnetization curves recorded at the maximum of the Tb x-ray reflectivity at $h\nu = 157$ eV are shown in Fig. 4(a) (open symbols). While the specular x-ray intensity is constant in the magnetically disordered phase, it changes monotonically with temperature in the ferromagnetic phase. The difference intensity amounts up to several μA of photocurrent which is easily measured with high accuracy, even by using a hand multimeter. We note that the two 157-eV branches in Fig. 4(a) are mirror images; thus unlike using visible light, already *a single branch* apparently yields the temperature dependent magnetization $M(T)$.

Furthermore, such accurate $M(T)$ data give access to fundamental magnetic quantities like, e.g., the critical exponent of the magnetization β, defined through $M(T)/M(0) = (1 - T/T_C)^{\beta}$. A closer inspection of the critical regime in Fig. 4(c) yields $\beta = 0.31 \pm 0.02$. It agrees with the theoretically expected value for a three-dimensional Ising system, indicating the presence of a substantial uniaxial magnetic anisotropy in the Tb metal film; it is likely to be induced by the bcc W(110) substrate of uniaxial symmetry.

With the present findings a future goal is now at reach. Intense x-ray beams from third-generation synchrotron radiation sources can be focused down to a few 10 nm spot size by Fresnel zone plates, utilized in several x-ray microscopes worldwide. So far a magnetic resolution of ~60 nm has been obtained using transparent samples suspended on organic foils [22]. The present discovery of strong MO signals from lanthanides opens the door to element specific microscopy studies using *reflectivity,* e.g., on the most relevant technological question about the switching behavior of heteromagnetic nanoscale systems [3,4] which are all prepared on *nontransparent* metal or semiconductor substrates.

It is a pleasure to thank Sven Bode for technical help and Paul Fumagalli for discussions. This work has been supported by the Bundesminister für Bildung und Forschung (05-SC8 KEB-6) and by the Deutsche Forschüngsgemeinschaft, SFB-290 (TPA6).

[1] D. S. Bloomberg and G. A. N. Connell, in *Magnetic Recording Handbook: Technology and Applications,* edited by C. D. Mee and E. D. Daniel (McGraw-Hill, New York, 1990).
[2] A. Hubert and R. Schäfer, *Magnetic Domains* (Springer, Berlin, Heidelberg, 1998).
[3] G. A. Prince, Science **282**, 1660 (1998).
[4] J. S. Jiang *et al.,* J. Appl. Phys. **83**, 6238 (1998); S. A. Majetich and Y. Jin, Science **284**, 470 (1999).
[5] D. Weller and W. Reim, Appl. Phys. A **49**, 599 (1989); Y. Takeno, K. Kaneko, and Y. Shimada, J. Magn. Soc. Jpn. **19**, S229 (1994).
[6] G. Schütz *et al.,* Phys. Rev. Lett. **58**, 737 (1987).
[7] C. T. Chen *et al.,* Phys. Rev. Lett. **75**, 152 (1995).
[8] J. Stöhr and R. Nakajima, IBM J. Res. Dev. **42**, 73 (1998).
[9] L. Tröger *et al.,* Phys. Rev. B **46**, 3283 (1992); C. T. Chen *et al., ibid.* **48**, 642 (1993).
[10] B. L. Henke, E. M. Gullikson, and J. C. Davis, At. Data Nucl. Data Tables **54**, 180 (1993).
[11] K. Starke *et al.,* Phys. Rev. B **55**, 2672 (1997); Eur. Phys. J. B **12**, 171 (1999) .
[12] H. A. Dürr *et al.,* Science **284**, 2166 (1999).
[13] C.-C. Kao *et al.,* Phys. Rev. B **50**, 9599 (1994); Y. U. Idzerda, V. Chakarian, and J. W. Freeland, Phys. Rev. Lett. **82**, 1562 (1999).
[14] J. Kolaczkiewicz and E. Bauer, Surf. Sci. **175**, 487 (1986); K. Starke, *Magnetic Dichroism in Core-Level Photoemission* (Springer, Berlin, Heidelberg, 2000).
[15] K. J. S. Sawhney *et al.,* Nucl. Instrum. Methods Phys. Res., Sect. A **390**, 395 (1997).
[16] M. Born and E. Wolf, *Principles of Optics* (Pergamon, London, 1959).
[17] R. D. Cowan, *The Theory of Atomic Structure and Spectra* (University of California Press, Berkeley, 1981).
[18] E. D. Tober *et al.,* Phys. Rev. B **53**, 5444 (1996).
[19] Magnetoelastic coupling is known to be large in lanthanide-based systems, where magnetostrictions can reach up to ~1% [A. E. Clark, in *Ferromagnetic Materials,* edited by E. P. Wohlfarth (North-Holland, Amsterdam, 1980), Vol. 1]. Thus, unlike most transition metals, thermal expansion of lanthanide lattices (metals and alloys) is strongly influenced by the temperature dependent "magnetostrains."
[20] The detailed description of the visible-light MO experiment will be given elsewhere.
[21] As in bulk Tb [J. Jensen and A. R. Mackintosh, *Rare Earth Magnetism Structures and Excitations* (Clarendon, Oxford, 1991), Sect. 5.7], we find that a helical magnetic phase exists within a few Kelvin below the ordering temperature; it is suppressed here by the external field.
[22] P. Fischer *et al.,* Z. Phys. B **101**, 313 (1996).